

Air–water CO₂ flux in an algae bloom year for Lake Hongfeng, Southwest China: implications for the carbon cycle of global inland waters

Faxiang Tao¹

Received: 15 January 2017/Revised: 18 June 2017/Accepted: 10 August 2017/Published online: 22 August 2017
© Science Press, Institute of Geochemistry, CAS and Springer-Verlag GmbH Germany 2017

Abstract The carbon cycle of global inland waters is quantitatively comparable to other components in the global carbon budget. Among inland waters, a significant part is man-made lakes formed by damming rivers. Man-made lakes are undergoing a rapid increase in number and size. Human impacts and frequent algae blooms lead to it necessary to make a better constraint on their carbon cycles. Here, we make a primary estimation on the air–water CO₂ transfer flux through an algae bloom year for a subtropical man-made lake—Hongfeng Lake, Southwest China. To do this a new type of glass bottles was designed for content and isotopic analysis of DIC and other environmental parameters. At the early stage of algae bloom, CO₂ was transferred from the atmosphere to the lake with a net flux of 1.770 g·C·m⁻². Later, the partial pressure (*p*CO₂) of the aqueous CO₂ increased rapidly and the lake outgassed to the atmosphere with a net flux of 95.727 g·C·m⁻². In the remaining days, the lake again took up CO₂ from the atmosphere with a net flux of 14.804 g·C·m⁻². As a whole, Lake Hongfeng released 4527 t C to the atmosphere, accounting for one-third of the atmosphere/soil CO₂ sequestered by chemical weathering in the whole drainage. With an empirical mode decomposition method, we found air temperature plays a major role in controlling water temperature, aqueous *p*CO₂ and hence CO₂ flux. This work indicates a necessity to make detailed and comprehensive carbon budgets in man-made lakes.

Keywords CO₂ flux · Algae bloom · Carbon cycle · Inland waters · Lake Hongfeng

1 Introduction

The carbon cycle in inland waters, including lakes, reservoirs, impoundments, rivers, and streams, is tightly associated with that in terrestrial ecosystems, the atmosphere and ocean ecosystems, and with human activities. By estimation, the carbon dioxide evaded from inland waters is about 2.1 Pg·C·year⁻¹ (Raymond et al. 2013), which is comparable to the ocean sink of 3.0 Pg C or to the land sink of 1.9 Pg C for year 2015 (Le Quéré et al. 2016). Thus, carbon dioxide dynamics from inland waters is a significant component of the global carbon cycle (Cole et al. 2007; Tranvik et al. 2009; Raymond et al. 2013).

Tropical and subtropical lakes are quite different from temperate lakes in terms of CO₂ dynamics (Marotta et al. 2009; Pinho et al. 2016). These waters and their catchments are characteristic of a major part of the world population, strong human activities, intensive monsoon rain impacts, origins of world main large rivers as well as increasing hydropower development activities. Man-made lakes and impoundments are continually increasing to meet enlarging power need gaps (Zarfl et al. 2015). Moreover, there is a general trend toward eutrophication for many inland waters in tropical and subtropical areas (Ansari and Gill 2014). Therefore, the carbon dioxide transfer from these waters is elusive and needs a better constraint.

Here, we present a dataset to describe the carbon dioxide dynamics during an algae bloom year for Lake Hongfeng (a man-made lake), Southwest China. The main goal of this study is to calculate air–lake CO₂ exchange flux and touch

✉ Faxiang Tao
taofaxiang@vip.gyig.ac.cn

¹ State Key Laboratory of Environmental Geochemistry, Institute of Geochemistry, Chinese Academy of Sciences, 99 Lincheng West Road, Guanshanhu District, Guiyang 550081, Guizhou, China

on the association of meteorological factors with aqueous CO_2 partial pressures.

2 Methods

2.1 Lake Hongfeng

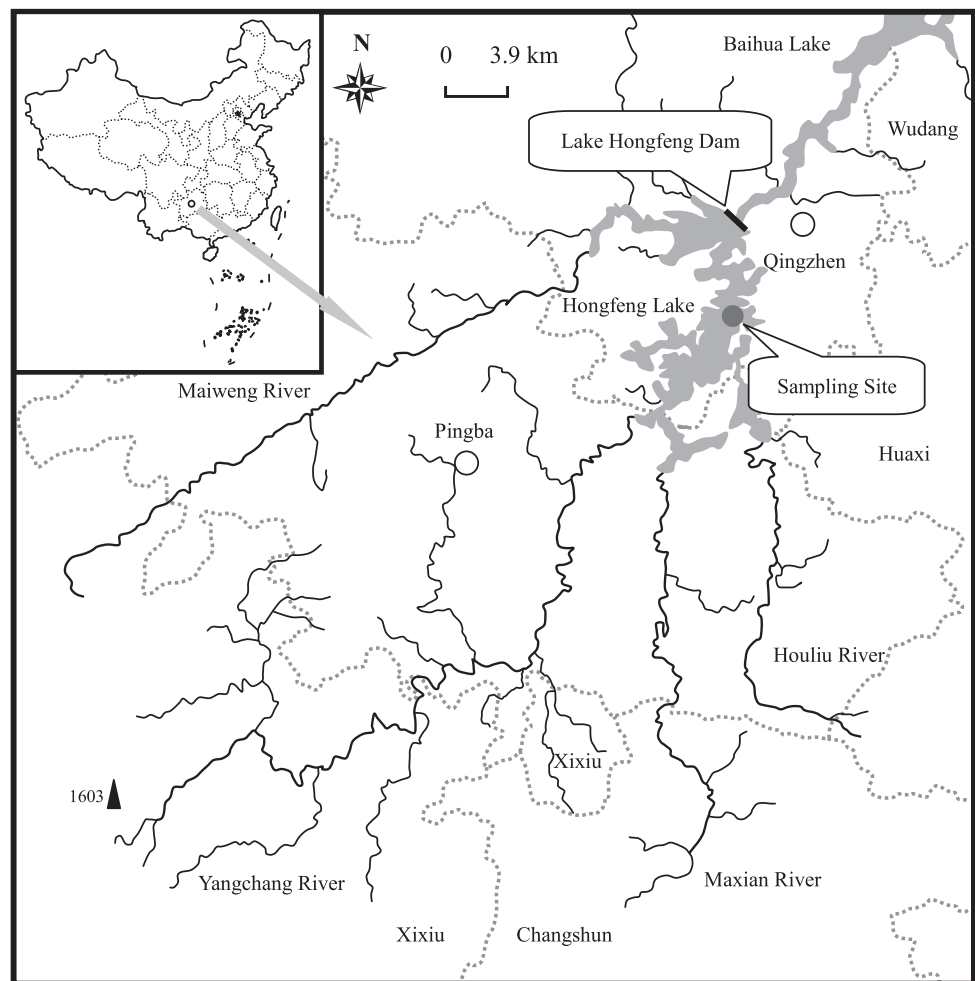
As a result of damming the Maotiao River, a tributary of the Wujiang River in the Yangtze River Basin, Lake Hongfeng was formed in 1960 for power generation, and drinking/industrial/agricultural water use (Fig. 1). It has a surface area of 57.2 km^2 ($26^\circ 26' \text{N}$ – $26^\circ 36' \text{N}$, $106^\circ 19' \text{E}$ – $106^\circ 28' \text{E}$) with a maximum length of 24 km and maximum breadth of 5 km. Its average depth is 10.5 m with a maximum depth of 45 m. The lake contains $6.01 \times 10^8 \text{ m}^3$ of water at its highest elevation of 1240 m above sea level while it has a dead storage of $1.59 \times 10^8 \text{ m}^3$ at an elevation of 1227.5 m. The water levels are 1228, 1237, 1233 and 1230 m for the low-water stage (DJF), rising-flood

stage (MAM), high-water stage (JJA) and falling-flood stage (SON), respectively (Yang et al. 2014). It annually collects $9.51 \times 10^8 \text{ m}^3$ of water from its drainage of 1596 km^2 . Lake Hongfeng has a retention time of about 0.325 years. Its watershed is influenced by the East Asian monsoon, with a hot and wet summer and a dry and cold winter (Fig. 2).

2.2 Sampling bottles

The content of dissolved inorganic carbon (DIC) in environmental waters is an essential parameter for the carbonic acid equilibrium-based calculation of the partial pressure of aqueous CO_2 and of the air–water CO_2 exchange flux. Now, a vacuum line is generally equipped in an isotope analysis lab. To use this line to synchronously determine the content and isotopic ratio of DIC, we have designed a new type of gas-tight glass bottles for in-site collection of water samples of any size (Fig. 3). In addition to their use in DIC analysis, these bottles can also be used for sampling

Fig. 1 Map showing Lake Hongfeng, its tributary systems and the sampling site. The inset indicates the relative location of Lake Hongfeng in China. Grey dotted lines are county boundaries



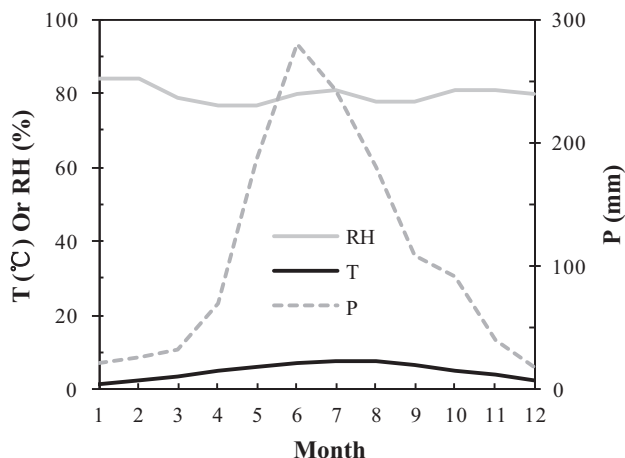


Fig. 2 Monthly mean temperature (T), precipitation (P) and relative humidity (RH) monitored at the Pingba Meteorological Station near Lake Hongfeng (See Fig. 1 for the location of Pingba)

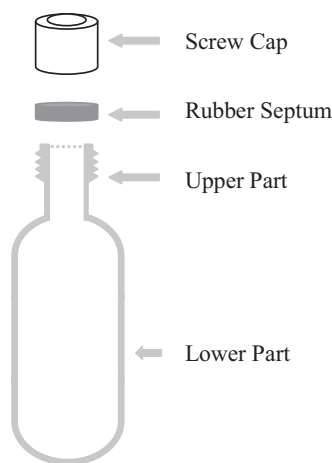


Fig. 3 Depiction of a new type of gas-tight glass bottles for DIC content and isotopic analysis as well as other uses in collecting air, soil, plant and water samples for content and isotopic analysis. The *upper part* of the bottle is made from a 4.5 mL round-bottomed borosilicate vial (Labco Limited, UK). The *lower part* is from a borosilicate tube of any diameter, depending upon a needed volume. Two parts were sealed by a glass blower. The total height of the bottle is 10 cm with a diameter of 2.8 or 4 cm for synchronous DIC content and ^{13}C analysis or for simultaneous DIC content, ^{13}C and ^{14}C analysis, respectively

soil, gas, air, and water for greenhouse gas and isotopic analysis. They can also be used for sampling soil and plants for water extraction and subsequent hydrogen/oxygen isotopic determination. In contrast to the medical glass septum tubes recommended by Atekwana and Krishnamurthy (1998), these bottles are characteristic of easy operation, reusability, rapid evasion of CO_2 due to low liquid level and large liquid surface, capability of storing enough water with low DIC content, and other broad applications in collecting various environmental samples.

2.3 Sampling and DIC analysis

An algae bloom event occurred in Lake Hongfeng in August of 2007. During the period from August 9 to September 3, 2007, water samples were collected daily near the drinking water intake site (Fig. 1). After that, the sampling frequency was lowered to a 1-day interval between September 7 and November 30, 2007. Finally, the sampling frequency was lowered to once a week between December 3, 2007 and January 7, 2008. Water samples were collected near the surface at two o'clock in the afternoon of each sampling day. Water temperature and pH values were measured on site with a portable multi-parameter tester—Pioneer[®] 65 (Radiometer Analytical, France).

For DIC analysis, 10 mL of water were injected on site into the above-mentioned bottle through a 20 mL syringe with a Hamilton needle (26S gauge). There was a 25 mm Swin-Lok[™] filter holder with a Whatman GF/F glass fibre filter (0.65 μm) positioned between the syringe and the needle. Each bottle was preloaded with 1 mL of 85% phosphoric acid (analytical grade) and a magnetic bar and evacuated to 4 Pa prior to water injection. The combination of septum and screw cap (Fig. 3) adequately guarantees gas tightness of sampling bottles. Parafilm wrapping between the screw cap and the bottle neck is of no use to stop the CO_2 in sampling bottles from evasion into the atmosphere. It is also notable that, in no case, the bottles with samples should be positioned upside down. If so, the phosphoric acid solution on the rubber septum would clog the needles upon puncture during CO_2 extraction.

In the lab, CO_2 was extracted in a vacuum line following the procedure of Atekwana and Krishnamurthy (1998); meanwhile its pressure and temperature were measured with a Barocel 600 pressure transducer (BOC Edwards, UK) and a digital thermometer (Ace Glass, USA), respectively. Thus, the DIC concentration could be obtained using the ideal gas law (scaled up to 1 L water):

$$n_g (\mu\text{M}) = P_g V_g / (RT_g)$$

$$\text{DIC} (\text{mM} \cdot \text{L}^{-1}) = n_g / V_s \cdot 1000 / 1000 = n_g / V_s$$

where, n_g is the number of micromoles for a gas (CO_2 gas in this experiment). P_g and T_g are the pressure (mbar) and absolute temperature (K) of CO_2 measured in the above-mentioned vacuum line, respectively. R is the ideal or universal gas constant ($R = 0.083145 \text{ mbar mL} \cdot \mu\text{M}^{-1} \cdot \text{K}^{-1}$). V_g is the fixed volume (13.2 mL for our vacuum line) of CO_2 captured in the pressure transducer assembly, and V_s is the volume (10 mL for this study) of a DIC sample. The figures (1000) in the numerator and in the denominator are volume (1 L = 1000 mL) and mole (1 mM = 1000 μM) conversion factors, respectively.

2.4 Data availability and processing

All meteorological data for the Pingba Meteorological Station (Fig. 1) cited in this work were downloaded from China Meteorological Data Network (<http://data.cma.cn/>). The monthly atmospheric CO₂ concentrations are available from an independent, citizen-led initiative through a web-site at <https://www.co2.earth/>.

The empirical mode decomposition (EMD) was utilized to decompose a time series into cyclical components and a long-term trend (Huang et al. 1998). Its upgraded version is called the complete ensemble empirical mode decomposition with adaptive noise (CEEMDAN) (Torres et al. 2011). CEEMDAN can be run on a computer through an R package (Luukko et al. 2016).

2.5 Calculation of CO₂ flux

2.5.1 Partial pressure of aqueous CO₂

In natural waters, DIC is mainly contributed to by three components: aqueous CO₂, carbonate, and bicarbonate (Butler 1982). Their concentration relationship can be described as:

$$\text{DIC} = [\text{CO}_2] + [\text{HCO}_3^-] + [\text{CO}_3^{2-}] \quad (1)$$

The dissolution of CO₂ in water can be represented with the following chemical and ionization equations:



In freshwaters, the activity of a species is approximate to its concentration. Thus, we have the following equations:

$$[\text{CO}_2] \times K_1 = [\text{HCO}_3^-] \times [\text{H}^+] \quad (2)$$

$$[\text{HCO}_3^-] \times K_2 = [\text{CO}_3^{2-}] \times [\text{H}^+] \quad (3)$$

The association between aqueous CO₂ concentration and its partial pressure (*p*CO₂ in atm) can be illustrated by Henry's law:

$$[\text{CO}_2] = K_H \times p\text{CO}_2 \quad (4)$$

K_H is the Henry's law constant in moles·L⁻¹·atm⁻¹. *K_H*, *K₁*, and *K₂* are temperature-dependent and can be estimated from empirical equations of Plummer and Busenberg (1982).

Thus, aqueous CO₂ contents and partial pressures can be obtained through Eqs. (1)–(4).

2.5.2 CO₂ flux

The CO₂ exchange across the air–water interface of a lake is tightly related with the CO₂ concentration gradient and the gas transfer velocity, *k* (in cm·h⁻¹). The former is also deterministic to the direction of CO₂ gas exchange and can be expressed as the difference between the actual concentration (*C_{aq}*) of CO₂ in the water and the concentration (*C_{eq}*) of CO₂ in the water at equilibrium with the overlying atmosphere. Then, combining Eq. (4), we have:

$$\text{Flux} = \varepsilon k (C_{\text{aq}} - C_{\text{eq}}) = \varepsilon k K_H (p\text{CO}_{2\text{aq}} - p\text{CO}_{2\text{air}}) \quad (5)$$

where ε is the chemical enhancement factor for CO₂ exchange. Here, we assume $\varepsilon \approx 1$ (See Sect. 4.1). *p*CO_{2_{aq} and *p*CO_{2_{air} are partial pressures of CO₂ in water and in air, respectively. *k* is related with *k₆₀₀* through the following equation (Jähne et al. 1987):}}

$$k_{600}/k_{\text{CO}_2} = (600/Sc_{\text{CO}_2})^{-0.5} \quad (6)$$

where, *k₆₀₀* is the value of *k* for CO₂ with a Schmidt number (*Sc*) of 600 in freshwater at 20 °C. It is not related to wind direction, rainfall, or relative humidity (Frost and Upstill-Goddard 2002). *k₆₀₀* is linked to the wind speed (*U₁₀* in m·s⁻¹) at 10 m above the water surface (Cole and Caraco 1998):

$$k_{600} = 2.07 + 0.215U_{10}^{1.7} \quad (7)$$

A *Sc* number (*Sc_{CO₂}*) for CO₂ in freshwater is associated with temperature through an empirical equation (Waninkhof 1992):

$$\begin{aligned} Sc_{\text{CO}_2} = & 1911.1 - 118.11t \\ & + 3.4527t^2 - 0.041320t^3 \quad (t \text{ in degrees Celsius}) \end{aligned} \quad (8)$$

The meteorological data at a height of 10 m above the lake surface were not available. The daily data at the Pingba Meteorological Station (Fig. 1) were used for the calculation of CO₂ flux covering the monitoring period (August to December of 2007) and for further analysis. The missing values for *p*CO₂ were obtained by linear interpolation. For the period from January to July of 2008, we used the relationship (*p*CO₂ = 6 × 10¹¹ × e^{-2.514pH}, R² = 0.993, n = 73) of pH with *p*CO₂ to infer the monthly mean partial pressure of CO₂, based on the pH and temperature (for *K_H* estimation) data monitored in 2009 (Xia et al. 2011).

Now, with Eqs. (5)–(8), we were able to get the CO₂ flux across the period from August of 2007 to July of 2008.

Table 1 Temperature (*T*), pH, contents of dissolved inorganic carbon (DIC), and calculated partial pressures of aqueous CO₂ for water samples collected in Lake Hongfeng during the period from August 9, 2007 to January 7, 2008

Sample no.	Date	<i>T</i> (°C)	pH	DIC (mM L ⁻¹)	<i>p</i> CO ₂ (ppm)	Sample no.	Date	<i>T</i> (°C)	pH	DIC (mM L ⁻¹)	<i>p</i> CO ₂ (ppm)
2007											
HFW01	Aug. 9	28.2	8.74	1.165	142.4	HFW38	Oct. 1	21.0	8.10	1.917	927.1
HFW02	Aug. 10	26.0	8.73	1.613	195.5	HFW39	Oct. 5	24.0	8.20	1.917	770.4
HFW03	Aug. 11	24.0	8.62	1.625	247.6	HFW40	Oct. 7	22.0	8.12	1.936	907.1
HFW04	Aug. 12	25.0	8.67	1.590	218.6	HFW41	Oct. 9	19.0	7.72	1.984	2185.7
HFW05	Aug. 13	26.4	8.96	1.556	109.9	HFW42	Oct. 11	21.0	7.83	2.038	1810.7
HFW06	Aug. 14	25.0	8.85	1.304	117.4	HFW43	Oct. 13	20.0	7.75	2.014	2106.9
HFW07	Aug. 15	28.0	8.85	1.229	115.5	HFW44	Oct. 15	17.5	7.34	2.116	5151.3
HFW08	Aug. 16	26.0	8.88	1.258	107.0	HFW45	Oct. 17	19.0	7.76	2.139	2157.1
HFW09	Aug. 17	26.0	8.86	1.485	132.4	HFW46	Oct. 19	19.0	8.01	2.168	1249.8
HFW10	Aug. 18	26.0	8.49	1.598	339.1	HFW47	Oct. 21	19.0	7.91	2.124	1533.6
HFW11	Aug. 19	22.1	8.57	1.472	245.3	HFW48	Oct. 23	20.0	7.43	2.149	4500.8
HFW12	Aug. 20	26.5	8.50	1.422	297.1	HFW49	Oct. 25	19.0	7.55	2.125	3392.4
HFW13	Aug. 21	24.2	8.64	1.236	180.2	HFW50	Oct. 27	19.0	7.87	2.047	1616.2
HFW14	Aug. 22	26.0	8.70	1.278	166.2	HFW51	Oct. 29	17.0	7.44	2.089	4096.0
HFW15	Aug. 23	23.0	8.67	1.350	180.5	HFW52	Oct. 31	17.0	7.41	2.088	4360.0
HFW16	Aug. 24	24.0	8.61	1.361	212.3	HFW53	Nov. 2	17.0	7.44	2.167	4249.3
HFW17	Aug. 25	24.0	8.59	1.543	252.1	HFW54	Nov. 4	12.0	7.46	2.095	3663.6
HFW18	Aug. 26	27.0	8.56	1.580	289.2	HFW55	Nov. 6	18.0	7.51	2.121	3636.3
HFW19	Aug. 27	26.0	8.71	1.251	158.9	HFW56	Nov. 8	18.0	7.50	2.014	3527.1
HFW20	Aug. 28	26.0	8.46	1.254	285.3	HFW57	Nov. 10	15.8	7.71	2.151	2315.1
HFW21	Aug. 29	27.0	8.25	1.296	485.8	HFW58	Nov. 12	17.0	8.08	1.889	904.1
HFW22	Aug. 30	26.0	8.50	1.380	286.1	HFW59	Nov. 14	17.0	8.11	1.578	705.5
HFW23	Aug. 31	26.0	8.48	1.403	304.7	HFW60	Nov. 16	18.0	7.97	2.137	1329.4
HFW24	Sept. 1	25.0	8.35	1.472	425.4	HFW61	Nov. 18	16.0	7.71	2.137	2306.8
HFW25	Sept. 2	24.0	8.00	1.482	939.0	HFW62	Nov. 20	16.0	7.61	2.163	2903.8
HFW26	Sept. 3	20.8	7.93	1.590	1126.1	HFW63	Nov. 22	11.0	7.63	2.155	2586.9
HFW27	Sept. 7	22.0	7.76	1.673	1762.2	HFW64	Nov. 24	18.0	7.55	2.170	3413.7
HFW28	Sept. 9	21.0	7.40	1.803	4084.4	HFW65	Nov. 26	16.0	7.58	2.191	3139.5
HFW29	Sept. 11	23.0	7.65	1.985	2705.7	HFW66	Nov. 28	16.0	7.62	2.221	2918.2
HFW30	Sept. 13	20.0	7.69	2.046	2443.5	HFW67	Nov. 30	16.0	7.66	2.189	2636.9
HFW31	Sept. 15	22.0	7.65	2.114	2838.9	HFW68	Dec. 3	16.0	7.61	2.206	2962.4
HFW32	Sept. 17	21.0	7.65	2.009	2657.5	HFW69	Dec. 10	15.0	7.63	2.212	2804.8
HFW33	Sept. 19	22.0	8.05	2.042	1121.6	HFW70	Dec. 17	14.2	7.58	2.233	3119.1
HFW34	Sept. 21	23.0	8.28	1.833	604.4	HFW71	Dec. 24	10.5	7.56	2.324	3221.4
HFW35	Sept. 25	21.0	7.76	2.005	2081.7	2008					
HFW36	Sept. 27	20.0	8.05	1.967	1050.0	HFW72	Jan. 2	6.0	7.46	2.320	3737.3
HFW37	Sept. 29	21.0	8.33	1.910	546.0	HFW73	Jan. 7	6.0	7.46	2.215	3567.1

HFW Hongfeng water

3 Results

3.1 *p*CO₂

Temperature, pH values, and measured DIC contents of all samples together with the calculated *p*CO₂ are listed in Table 1.

The mean concentration of atmospheric CO₂ was 384.9 ± 2.7 ppm with a range of 381.0–388.5 ppm from August of 2007 to July of 2008. Based on these data, the evolution of *p*CO₂ for Lake Hongfeng can be divided into two stages (Table 1). The first stage started on August 9 and ended on the last day of August, with *p*CO₂ lower than that in the atmosphere (Fig. 4). The second one began on

September 1, 2007 and continued to the next year 2008, with $p\text{CO}_2$ higher than that in the atmosphere.

Consequently, in the first stage, CO_2 was transferred from the atmosphere to Lake Hongfeng, and during the second stage CO_2 was transported from Lake Hongfeng to the atmosphere. The partial pressure of CO_2 varied between 107.0 and 485.8 ppm with a mean value of 220.4 ± 91.5 ppm ($n = 23$) and between 425.4 and 5151.3 ppm with a mean value of 2416.0 ± 1216.6 ppm ($n = 50$) during the first stage and the second stage, respectively. In the whole monitoring period, the partial pressure of CO_2 in Lake Hongfeng presented distinct fluctuations and an obvious increasing trend (Fig. 4).

3.2 CO_2 flux

From August of 2007 to July of 2008, the monthly CO_2 flux covered a range of -3.42 to $33.06 \text{ g}\cdot\text{m}^{-2}$ with a mean value of $6.60 \pm 13.17 \text{ g}\cdot\text{m}^{-2}$ (Fig. 5). It is clear that the CO_2 flux from Lake Hongfeng to the atmosphere is much higher than that from the atmosphere to Lake Hongfeng. The net annual flux is up to $79.15 \text{ g}\cdot\text{m}^{-2}$.

With no considerations on changes in water level caused by precipitation or artificial regulations, we scaled up this annual flux to the whole lake (57.2 km^2) so that the annual net flux of CO_2 from Lake Hongfeng to the atmosphere accounted for $4.527 \times 10^9 \text{ g C}$ or 4527 t C .

This flux is a very conservative estimation, based on the following considerations. First, the pH data for months of January to July of 2008 was unavailable, and the data monitored in 2009 were used as a substitute. The latter had

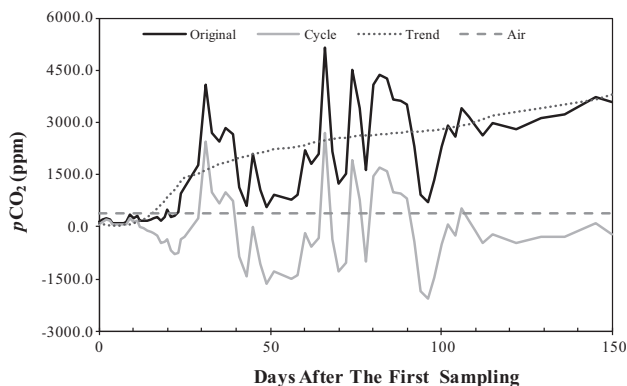


Fig. 4 Partial pressure ($p\text{CO}_2$) of aqueous CO_2 during the sampling period (The first sampling is on Aug. 9, 2007). With the CEEMDAN method, the original time series was decomposed into a cyclical component (Cycle) and a long-term trend (Trend). For the decomposition, the number of 4 is used to stop the EMD procedure. The maximum number of ensemble size is 250. The maximum number of 50 is used for stopping siftings. The value of 0.2 relative to the standard deviation of the input signal is used as additional noise. The horizontal line (Air) is the mean partial pressure (384.9 ppm) of the atmosphere CO_2 during the period from August of 2007 to July of 2008

very high pH values and changed in a narrow pH span of 8.29–9.09 with a mean value of 8.73 ± 0.28 . Second, the boundary layer gas transfer method used in this work generally has an underestimation (Anderson et al. 1999; Jonsson et al. 2008) or congruent (Eugster et al. 2003) estimation of CO_2 flux compared to the eddy covariance technique. Finally, we do not consider the alterations in CO_2 transfer velocity during night. The nighttime CO_2 transfer velocities could be enhanced due to water side convection, and hence an elevated CO_2 flux should be expected (Podrajsek et al. 2016).

4 Discussion

4.1 Chemical enhancement of CO_2 exchange

Air-lake transfer of CO_2 can be enhanced chemically by the hydration or dehydration reactions of CO_2 with hydroxide ions and water molecules (Wanninkhof 1992; Wanninkhof and Knox 1996). These reactions or processes are also called chemically enhanced diffusion (CED) and may be catalyzed by carbonic anhydrase. CED plays a more important role in the CO_2 exchange across the air-lake interface at low winds ($<5 \text{ m}\cdot\text{s}^{-1}$) and in eutrophic lakes with high pH, and hence may exert an influence on the estimation of CO_2 exchange flux.

During the period from August of 2007 to July of 2008, almost all daily winds (with two outliers) were located in this low wind interval. Therefore, the chemical enhancement may distort our estimation. However, the recent work by Bade and Cole (2006) shows that CED is accompanied with chemically enhanced fractionation (CEF) of carbon isotopes. CEF will lead to DIC with very low or more negative carbon isotope ratios. CEF can alter the carbon isotopic signal ($\delta^{13}\text{C}$) of DIC from -9% to -21% (Bade and Cole 2006). But for Lake Hongfeng we did not capture

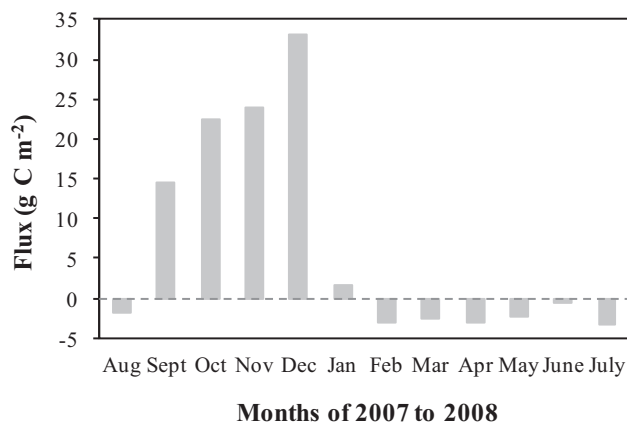


Fig. 5 Monthly CO_2 flux from August of 2007 to July of 2008

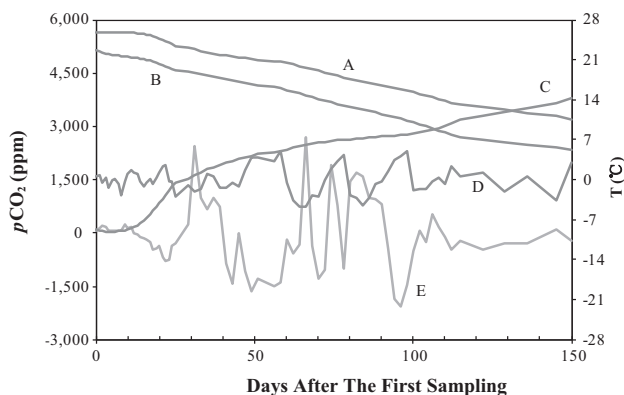


Fig. 6 Relationship of air temperature with water temperature and the partial pressure ($p\text{CO}_2$) of aqueous CO_2 in the sampling period (The first sampling is on Aug. 9, 2007). Air or water temperature time series was also decomposed into a cyclical component (Cycle) and a long-term trend (Trend). The parameters applied in the CEEMDAN method are the same as those in Fig. 4. A Water T Trend. B Air T Trend. C $p\text{CO}_2$ Trend. D Air T Cycle. E $p\text{CO}_2$ Cycle

this CEF signal as DIC $\delta^{13}\text{C}$ values of all samples are near -9‰ (unpublished data). Thus, the CED effect may be negligible in our CO_2 flux estimation.

4.2 Controls of air temperature on water temperature and $p\text{CO}_2$

In monsoon areas, air temperature is controlled by monsoon circulations. It is a main driving force for changes in water temperature and $p\text{CO}_2$ (Fig. 6). The long-term trend of water temperature is almost identical to that of air temperature (see curves A and B in Fig. 6: $r = 0.999$, $n = 73$, $p < 0.001$).

Moreover, it is interesting that air temperature played a more important role in controlling the evolution of $p\text{CO}_2$. Its long-term trend is significantly related to that of $p\text{CO}_2$ (see curves B and C in Fig. 6: $r = -0.943$, $n = 73$, $p < 0.001$). Meanwhile, the cyclical components of air temperature have a contribution of 27% to the fluctuations of $p\text{CO}_2$ (see curves D and E in Fig. 6: $r = -0.516$, $n = 73$, $p < 0.001$). In contrast, water temperature only has a contribution of 7% to the cyclical components of $p\text{CO}_2$ ($r = -0.268$, $n = 73$, $p < 0.05$). It is notable that there is a temporal negative relationship of temperature with $p\text{CO}_2$ in this study while there is a spatial positive relationship between temperature and $p\text{CO}_2$ present across different climate zones in the Northern Hemisphere (Marotta et al. 2009).

4.3 Implications for the carbon budget of global inland waters

Lake Hongfeng is a typical lake in tropical and subtropical areas. Its watershed is underlain mainly by carbonate rocks.

Globally, exposed carbonate rocks account for 13.4% of the continents surface, ranking fourth just after shield rocks (27.6%), sands and sandstones (26.3%), and shales (25.3%) (Amiotte-Suchet et al. 2003). In subtropical areas, their distribution is more than 25%. Carbonate rocks have a contribution of 24.4% in the total CO_2 consumed by the chemical weathering of all rock types (Hartmann et al. 2009). The virtual number for this value (24.4%) will be much higher due to the chemical weathering of carbonate minerals contained in non-carbonate rocks (Blum et al. 1998). Input of inorganic carbon (mainly in the form of bicarbonate HCO_3^-) produced by the chemical weathering of carbonate rocks is a predominant driver for CO_2 outgassing from global inland waters (McDonald et al. 2013; Marcé et al. 2015). Moreover, Lake Hongfeng has a mean pH of 8.43 with a scope of 7.37–9.00 during the period of 2006–2008 (Guiyang Municipal Bureau of Environmental Protection 2009), well inside the pH range of 7.3–9.2 for global freshwater lakes (Nikanorov and Brazhnikova 2002).

The quantity and water surface area of man-made lakes by damming rivers have been rapidly increasing due to clean energy and drinking/irrigation needs. Their emergence exerts a significant impact on the global carbon cycle.

A man-made lake provides a site to transform or process carbon species such as DIC species formed mainly by chemical weathering. For instance, thinking of the $9.51 \times 10^8 \text{ m}^3$ of water annually collected by Lake Hongfeng, we could get a DIC flux of $2.853 \times 10^{10} \text{ g C}$, given a mean DIC content of $2.5 \text{ mM}\cdot\text{L}^{-1}$. Generally, half this carbon, e.g. $1.427 \times 10^{10} \text{ g C}$, is expected to come from the atmosphere or soil CO_2 taken up during chemical weathering. Thus, the outgassed carbon from Lake Hongfeng can account for one-third of this atmosphere/soil carbon sequestered by chemical weathering. In many rivers, such as the Maotiao River in this work, step man-made lakes are constructed and carbon species will be continually reprocessed in these lakes on their way to the ocean. In order to balance the global carbon budget, humans must make new efforts to search for new carbon sinks to offset the carbon released from these man-made lakes.

Carbon cycles in man-made lakes located in tropical/subtropical areas are frequently disturbed by algae blooms. Since 1996 at least nine algae bloom events have occurred in Lake Hongfeng (Table 2). Damming rivers have also transformed the flows of rivers and altered their carbon-releasing/-uptake pathways. A better constraint on the carbon cycle of global inland waters is needed in terms of their role in greenhouse gas emission both at a global scale (Goldenfum 2012) and at a landscape level (Premke et al. 2016), or in terrestrial carbon accounting (Butman et al. 2016). A clear carbon budget on global inland waters

Table 2 Algae bloom events for Lake Hongfeng since 1996

Year	Month	Year	Month
1996	June	2005	August
1997	March	2006	August
1998	March	2007	August
1999	June	2008	August
		2015	July

is still an onerous task for the scientific community (Deemer et al. 2016). As the carbon evaded from global inland waters is a significant part in the global carbon cycle, then the question is what biogeochemical processes are responsible for balancing this carbon?

5 Conclusions

We have designed a new type of glass bottles to allow for on-site collection of environmental water for DIC content analysis and then for the calculation of the partial pressure of aqueous CO₂ and of the air–water CO₂ exchange flux. These bottles worked well in this study.

It is found that only at the early stage of this algae bloom, the CO₂ in Lake Hongfeng was undersaturated with respect to that in the atmosphere. As a whole even in an algae bloom year, Lake Hongfeng is still a source of the atmospheric CO₂ in terms of air–water CO₂ exchange. By a conservative estimation, it annually releases at least 4527 t C to the atmosphere.

Air temperature is a main factor controlling water temperature and the partial pressure of aqueous CO₂, based on an upgraded empirical mode decomposition method. Its long-term trend and cyclical components are significantly correlated with those of water temperature and the partial pressure of aqueous CO₂.

The outgassed CO₂ from Lake Hongfeng is equal to one-third of the carbon dioxide sequestered by chemical weathering in the whole drainage. Further research is needed to identify which biogeochemical processes are responsible for DIC supply. The work also shows that a comprehensive and detailed carbon budget is necessary in order to ascertain if Lake Hongfeng as a whole is a carbon source or a carbon sink.

Acknowledgements This work was carried out with funding from the National Key Research and Development Project provided by the Ministry of Science and Technology of China through Grant 2016YFA0601000. Two anonymous referees provided constructive comments and suggestions on the early version of the manuscript. F. Tao was very helpful for in-lab DIC analysis. Field sampling was assisted by Guiyang Municipal Institute of Environmental Protection. We are debt to J. Rui and Q. Yuan for their suggestions on the use of R packages.

References

- Amiotte-Suchet P, Probst J-L, Ludwig W (2003) Worldwide distribution of continental rock lithology: implications for the atmospheric/soil CO₂ uptake by continental weathering and alkalinity river transport to the oceans. *Glob Biogeochem Cycles* 17:45–56
- Anderson DE, Streigl RG, Stannard DI, Michmerhuizen CM, McConnaughey TA, LaBaugh JW (1999) Estimating lake-atmosphere CO₂ exchange. *Limnol Oceanogr* 44:988–1001
- Ansari AA, Gill SS (2014) *Eutrophication: causes, consequences and control*, vol 2. Springer, London
- Atekwana A, Krishnamurthy RV (1998) Seasonal variations of dissolved inorganic carbon and δ¹³C of surface waters: application of a modified gas evolution technique. *J Hydrol* 205:265–278
- Bade DL, Cole JJ (2006) Impact of chemically enhanced diffusion on dissolved inorganic carbon stable isotopes in a fertilized lake. *J Geophys Res* 111:C01014. doi:10.1029/2004JC002684
- Blum JD, Gazis CA, Jacobson AD, Chamberlain CP (1998) Carbonate versus silicate weathering in the Raikhot watershed within the High Himalayan Crystalline Series. *Geology* 26:411–414
- Butler JN (1982) *Carbon dioxide equilibria and their applications*. Addison-Wesley Publishing Company Inc, London
- Butman D, Stackpoole S, Stets E, McDonald CP, Clow DW, Striegl RG (2016) Aquatic carbon cycling in the conterminous United States and implications for terrestrial carbon accounting. *PNAS* 113:58–63
- Cole JJ, Caraco NF (1998) Atmospheric exchange of carbon dioxide in a low-wind oligotrophic lake measured by the addition of SF₆. *Limnol Oceanogr* 43:647–656
- Cole JJ, Prairie YT, Caraco NF, McDowell WH, Tranvik LJ, Striegl RG, Duarte CM, Kortelainen P, Downing JA, Middelburg JJ, Melack J (2007) Plumbing the global carbon cycle: integrating inland waters into the terrestrial carbon budget. *Ecosystems* 10:171–184
- Deemer BR, Harrison JA, Li S, Beaulieu JJ, Delsontro T, Barros N, Bezerra-Neto JF, Powers SM, Santos MAD, Vonk JA (2016) Greenhouse gas emissions from reservoir water surfaces: a new global synthesis. *Bioscience* 66:949–964. doi:10.1093/biosci/biw117
- Eugster W, Kling G, Jonas T, McFadden JP, Wuest A, McIntyre S, Chapin FS III (2003) CO₂ exchange between air and water in an Arctic and midlatitude Swiss lake: importance of convective mixing. *J Geophys Res* 108(D12):4362. doi:10.1029/2002JD002653
- Frost T, Upstill-Goddard RC (2002) Meteorological controls of gas transfer exchange at a small English lake. *Limnol Oceanogr* 47:1165–1174
- Goldenfum JA (2012) Challenges and solutions for assessing the impact of freshwater reservoirs on natural GHG emissions. *Ecohydrol Hydrol* 12:115–122
- Guiyang Municipal Bureau of Environmental Protection (2009) *Guiyang environmental quality reports 2006/2007/2008 (unpublished documents in Chinese)*
- Hartmann J, Jansen N, Dürr HH, Kempe S, Köhler P (2009) Global CO₂-consumption by chemical weathering: what is the contribution of highly active weathering regions? *Glob Planet Change* 69:185–194
- Huang NE, Shen Z, Long SR, Wu MC, Shih HH, Zheng Q, Yen N-C, Tung CC, Liu HH (1998) The empirical mode decomposition and the Hilbert spectrum for nonlinear and non-stationary time series analysis. *Proc R Soc (A)* 454:903–995

- Jähne B, Münnich KO, Börsinger R, Dutzi A, Huber W, Libner P (1987) On the parameters influencing air-water gas exchange. *J Geophys Res* 92:1937–1949
- Jonsson A, Åberg J, Lindroth A, Jansson M (2008) Gas transfer rate and CO₂ flux between an unproductive lake and the atmosphere in northern Sweden. *J Geophys Res* 113:G04006. doi:10.1029/2008JG000688
- Le Quéré C, Andrew RM, Canadell JG et al (2016) Global carbon budget 2016. *Earth Syst Sci Data* 8:605–649
- Luukko PJJ, Helske J, Räsänen E (2016) Introducing libeemd: a program package for performing the ensemble empirical mode decomposition. *Comput Stat* 31:545–557
- Marcé R, Obrador B, Morgui J-A, Rilar JL, López P, Armengol J (2015) Carbonate weathering as a driver of CO₂ supersaturation in lakes. *Nat Geosci* 8:107–111
- Marotta H, Duarte CM, Sobek S, Enrich-Prast A (2009) Large CO₂ disequilibria in tropical lakes. *Glob Biogeochem Cycles* 23:GB4022. doi:10.1029/2008GB003434
- McDonald CP, Stets EG, Striegl RG, Butman D (2013) Onorganic carbon loading as a primary driver of dissolved carbon dioxide concentrations in the lakes and reservoirs of the contiguous United States. *Glob Biogeochem Cycles* 27:285–295
- Nikanorov AM, Brazhnikova Lü (2002) Water chemical composition of rivers, lakes and wetlands. In: Types and properties of water - Vol. II. Encyclopedia of life support systems (EOLSS). Eolss Publishers Co. Ltd. <http://www.eolss.net/sample-chapters/c07/e2-03-04-02.pdf>
- Pinho L, Duarte CM, Marotta H, Enrich-Prast A (2016) Temperature dependence of the relationship between pCO₂ and dissolved organic carbon in lakes. *Biogeosciences* 13:865–871
- Plummer LN, Busenberg E (1982) The solubilities of calcite, aragonite and vaterite in CO₂-H₂O solutions between 0 and 90 C, and an evaluation of the aqueous model for the system CaCO₃-CO₂-H₂O. *Geochim Cosmochim Acta* 46:1011–1040
- Podrajsek E, Sahlee E, Rutgersson A (2016) Enhanced nighttime gas emissions from a lake. In: The 7th international symposium on gas transfer at water surfaces. IOP conference series: earth environmental science, vol 35. doi:10.1088/1755-1315/35/1/012014
- Premke K, Attermeier K, Augustin J, Cabezas A, Casper P, Deumlich D, Gelbrecht J, Gerke HH, Gessler A, Grossart H-P, Hilt S, Hupfer M, Kalettka T, Kayler Z, Lischeid G, Sommer M, Zak D (2016) The importance of landscape diversity for carbon fluxes at the landscape level: small-scale heterogeneity matters. *WIREs Water* 3:601–617
- Raymond P, Hartmann J, Lauerwald R, Sobek S, McDonald C, Hoover M, Butman D, Striegl R, Mayorga E, Humborg C, Kortlainen P, Dürr H, Meybeck M, Ciais P, Guth P (2013) Global carbon dioxide emissions from inland waters. *Nature* 503:355–359
- Torres ME, Colominas MA, Schlotthauer G, Flandrin P (2011) A complete ensemble empirical mode decomposition with adaptive noise. In: Proceedings of the 2011 IEEE international conference on acoustics, speech and signal processing (ICASSP), pp 4144–4147
- Tranvik LJ, Downing JA, Cotner JB et al (2009) Lakes and reservoirs as regulators of carbon cycling and climate. *Limnol Oceanogr* 54:2298–2314
- Wanninkhof R (1992) Relationship between wind speed and gas exchange over the ocean. *J Geophys Res* 97:7373–7387
- Wanninkhof R, Knox M (1996) Chemical enhancement of CO₂ exchange in natural waters. *Limnol Oceanogr* 41:689–697
- Xia P, Lin T, Li C, Xue F, Zhang B, Jiang Y (2011) Response of the water quality to seasonal stratification in Lake Hongfeng, China. *Environ Sci* 31:1477–1485 (in Chinese with English abstract)
- Yang T, Liu H, Yu Y (2014) Water quality trend and possible causes for Lake Hongfeng. *Resour Environ Yangtze Basin* 23(S1):96–102 (in Chinese with English abstract)
- Zarfl C, Lumsdon AE, Berlekamp J, Tydecks L, Tockner K (2015) A global boom in hydropower dam construction. *Aquat Sci* 77:161–170